Near-infrared refractive index of synthetic single crystal and polycrystalline diamonds at high temperatures

Article *in* Journal of Applied Physics · December 2017

DOI: 10.1063/1.5008387

CITATIONS
0

READS
122

6 authors, including:

V.Yu. Yurov
Russian Academy of Sciences
48 PUBLICATIONS **465** CITATIONS

SEE PROFILE

Near-infrared refractive index of synthetic single crystal and polycrystalline diamonds at high temperatures

V. Yu. Yurov, E. V. Bushuev, A. F. Popovich, A. P. Bolshakov, E. E. Ashkinazi, and V. G. Ralchenko

Citation: Journal of Applied Physics **122**, 243106 (2017);
View online: https://doi.org/10.1063/1.5008387
View Table of Contents: http://aip.scitation.org/toc/jap/122/24
Published by the American Institute of Physics

Near-infrared refractive index of synthetic single crystal and polycrystalline diamonds at high temperatures

V. Yu. Yurov,[1,2,a)] E. V. Bushuev,[1] A. F. Popovich,[1,3] A. P. Bolshakov,[1,2,4] E. E. Ashkinazi,[1,2] and V. G. Ralchenko[1,2,4]
[1]*General Physics Institute of Russian Academy of Sciences, Moscow 119991, Russia*
[2]*National Research Nuclear University «MEPhI», Moscow 115409, Russia*
[3]*Institute of Radio Engineering and Electronics, Russian Academy of Sciences, Fryazino 141190, Russia*
[4]*Harbin Institute of Technology, Harbin 150080, People's Republic of China*

(Received 5 October 2017; accepted 9 December 2017; published online 29 December 2017)

We measured the refractive index $n(T)$ and thermo-optical coefficient $\beta(T) = (1/n)(dn/dT)$ of high quality synthetic diamonds from room temperature to high temperatures, up to 1520 K, in near-infrared spectral range at wavelength 1.56 μm, using a low-coherence interferometry. A type IIa single crystal diamond produced by high pressure–high temperature technique and a transparent polycrystalline diamond grown by chemical vapor deposition were tested and revealed a very close $n(T)$ behavior, with $n = 2.384 \pm 0.001$ at $T = 300$ K, monotonically increasing to 2.428 at 1520 K. The $n(T)$ data corrected to thermal expansion of diamond are well fitted with 3rd order polynomials, and alternatively, with the Bose-Einstein model with an effective oscillator frequency of 970 cm^{-1}. Almost linear $n(T)$ dependence is observed above 800 K. The thermo-optical coefficient is found to increase monotonically from $(0.6 \pm 0.1) \times 10^{-5} K^{-1}$ (300 K) to $(2.0 \pm 0.1) \times 10^{-5} K^{-1}$ (1300 K) with a tendency to saturation at >1200 K. These $\beta(T)$ values are an order of magnitude lower than those known for Si, GaAs, and InP. The obtained results significantly extend the temperature range, where the refractive index of diamond was previously measured. *Published by AIP Publishing.*
https://doi.org/10.1063/1.5008387

I. INTRODUCTION

Due to excellent mechanical, thermal, and optical properties, single crystal (SC) and polycrystalline diamond grown by the chemical vapor deposition (CVD) technique is a valuable material for advanced optical applications, such as Raman lasers,[1,2] X-ray optics,[3,4] windows for high power IR lasers[5,6] and MW power class gyrotrons,[7] photonic crystals,[8,9] and quantum optics devices.[10] Diamond has a high refractive index, $n = 2.4$ at room temperature in the visible range, which increases with temperature.[11,12] The dependence $n(T)$ is important in the analysis of laser interaction with diamond, in particular, in the case of ultrashort pulse irradiation used to form localized buried graphite structures[13] or create color centers, such as nitrogen-vacancy defects,[14] when a very high local temperature, up to diamond-graphite transition above 1700 °C can be achieved. In the technology of CVD, diamond growth or etching the data on $n(T)$ for diamond in the temperature rate 700–1300 °C are necessary to monitor precisely *in situ* the evolution of diamond crystal thickness with the time of the process.[15,16]

Recently, a trend to go to a higher diamond deposition temperature in microwave plasma CVD (MPCVD) is observed due to a possibility of increasing the growth rate significantly.[16,17] Even higher temperatures, above 1700 K, are used for post-growth low-pressure/high-temperature (LPHT) annealing of diamond crystals in pure H_2 microwave plasma to reduce the defects concentration or modify the defects structure, thus to enhance the diamond color.[18] The crystal thickness monitoring during the LPHT process could be a valuable tool to establish safe (without mass loss) treatment regimes. In view of the technological relevance of diamond in high-temperature applications, a precise measurement of its refractive index in this regime is important.

However, the literature data on the experimental values $n(T)$ above 600 °C are quite scarce, and, to our best knowledge, there are no data available above 1000 °C. Moreover, since the refractive index has a spectral dispersion, it is difficult to compare the published data, as they often refer to different wavelengths. Ruf *et al.*[12] measured the temperature dependence of the refractive index of type II natural diamond up to 925 K at wavelength $\lambda = 100$ μm using an interferometric method, and fitted the obtained $n(T)$ dependence with a Bose-Einstein (BE) model. Tropf *et al.*[19] interferometrically studied the $n(T)$ for polycrystalline diamond films over a broad spectral infrared range (2.2–10 μm) at $T = 20$–511 °C, while Hu and Hess[20] determined the optical constants of a nanocrystalline diamond (NCD) film using ellipsometry in the UV-vis-NIR spectral range at T = 30–500 °C. To our best knowledge, only in two works, the refractive index and/or thermo-optical coefficient were/was determined for diamond at temperatures above 1000 K. Patterson[21] measured the values $dn/dT(T)$ and $(1/n)(dn/dT)$ for different sorts of diamond [natural Ia, IIa, and IIb types and synthetic high pressure–high temperature (HPHT) type Ib] with an interferometer in the visible spectrum at wavelengths 632.8 and 488.0 nm at temperatures 300–1300 K; however, no data on $n(T)$ were reported. Zouboulis *et al.*[22] measured $n(T)$ for single crystal diamond (supposedly natural diamond) from 300 to 1600 K

a)Author to whom correspondence should be addressed: yurov6591@gmail.com

using Brillouin scattering at an excitation wavelength of 514.5 nm. Their data, however, seem to be not accurate enough, especially at high temperatures; for example, the value $n = 2.51 \pm 0.03$ can be deduced for T = 1500 K from the presented plot (see Fig. 3 in Ref. 22) and no estimate of $(1/n)(dn/dT)$ was given. A review of temperature dependent $n(T)$ for diamond can be found in Refs. 23 and 24.

Here, we determined the temperature dependent refractive index and thermo-optical coefficient $(1/n)(dn/dT)$ for two sorts of synthetic diamond, type IIa single crystal HPHT diamond and optical quality polycrystalline CVD diamond, at temperatures from 300 K to 1520 K, well beyond 1000 K explored before. These optical properties were measured at a wavelength of 1.56 μm using a low-coherence interferometry (LCI), applied by us before for the *in situ* study of diamond growth kinetics in a microwave plasma.[15,16]

II. EXPERIMENTAL

A. Samples

One of the samples was a highly pure commercial type IIa single crystal diamond HTHT (NDT Ltd.)[25] with dimensions $\approx 4 \times 4 \times 0.9\,\text{mm}^3$, with large facets of (100) orientation, polished to the surface roughness R_a below 5 nm as measured with an optical profilometer (ZYGO NewView5000), and nonparallelism of 4 μm/mm. The thickness $d = 919 \pm 2$ μm in the central part of the plate was determined with a mechanical micrometer with an accuracy of 1 μm. A nitrogen impurity concentration of less than 5 ppb has been assessed from UV (270 nm) absorption intensity for this sample.

The second sample was a commercial transparent optical quality polycrystalline CVD diamond disk of 8 mm in diameter and thickness $d = 473 \pm 1$ μm in the central part of the disk (Element Six, Ltd.)[26] with a nitrogen content of $\approx$1 ppm, polished from both sides to the surface roughness $R_a < 15$ nm, with nonparallelism of 0.6 μm/mm. The typical grain size of about 30 μm on the growth side and 9 μm on the substrate side of the polycrystalline specimen was evaluated upon inspection with an optical microscope.

B. Measurement procedure

The laboratory stand for optical properties measurement at elevated temperatures is shown in Fig. 1. The sample was placed in an alumina holder inside a quartz tube in the central part of a furnace, with a large face perpendicular to longitudinal axis with an accuracy of about 0.5° that was controlled by monitoring the spot reflection position at an objective aperture. As diamond is known to be subjected to a noticeable etching in air at temperatures above approximately 600 °C, the quartz tube was evacuated to a pressure of $\approx 10^{-6}$ Torr to prevent the oxidation at elevated temperatures. The temperature of the diamond specimen was measured by an S-type thermocouple (Pt/Pt + 10%Rh) positioned in proximity of its rear side center.

The product of refractive index by the sample thickness $nd(T)$ was measured with a low-coherence Michelson tandem type interferometer (LCI); its principle of work was described elsewhere.[15] In brief, the beam of the low-coherence infrared

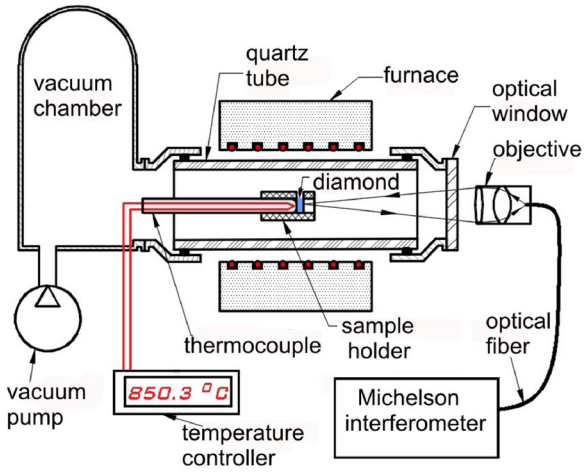

FIG. 1. Schematics of the stand for measurement of refractive index of diamond (see the text for details).

radiation from a superluminescent diode (SLD) at $\lambda = 1.56$ μm wavelength with a broad bandwidth $\Delta\lambda = 30$ nm passes through the Michelson interferometer (MI), splitting into two beams reflected from fixed and scanning (back-and-forth @1 Hz) mirrors. Then, the beams are directed perpendicularly to the diamond plate surface through an objective positioned near the quartz window of the furnace tube. These beams reflecting from the front and back surfaces of the diamond plate, which itself is an interferometer, return to a photodetector (PD) through an objective and an optical fiber. Due to a short coherence length ($L_{coh} \approx 30$ μm), only a limited number of interference fringes (about 20–30 fringes) arise in the PD. The interference pattern, detected as Gaussian-like envelope (0.75 ms duration) of fringes in the time-dependent PD output signal, occurs only at certain MI scanning mirror displacements, which provide the equality of optical paths between the mirrors inside MI and between the front and back planes of the sample plate. The optical thickness nd is measured from the time delay between the interference signals (envelopes), or more accurately, from the fine structure within the envelope. The increment $[nd(T) - nd(300)]$ relative to the initial value $nd(300)$ at $T = 300$ K is determined with a higher accuracy from the fine structure formed by the interference fringes (phase shift beating in time) between the two beams reflected from the scanning and fixed mirrors. The measured area was chosen in the sample center, and the diameter of the probed area (illuminated by the SLD) was about 40 μm.

The nd values were collected with a frequency of $\approx$0.3 Hz. The sample temperature was increased in steps of 50 K, recording the nd value at each step. As both $n(T)$ and $d(T)$ values are sensitive to the temperature fluctuations, in order to increase the accuracy, the measurements were performed only after the stabilization of the new temperature level. Then, the refractive index was calculated $n(T) = nd(T)/d(T)$, where $d(T) = d_0(1 + \langle\alpha\rangle T)$, $\langle\alpha\rangle(T)$ is the integrated thermal expansion coefficient $\alpha(T)$ over the temperature range from 300 K to T. We used the tabulated data for $\alpha(T)$ from Ref. 27, as the most reliable source, then fitted with a 3rd order polynomial, and integrated the polynomial to the given T to obtain $\langle\alpha\rangle = (1/T)\int\alpha(T)\delta T$. As the published

experimental data for $\alpha(T)$ show a considerable spread above ~1000 K (see Ref. 27 for a review), the error in the refractive index measurement is caused to a large extent by an error in the adopted $\alpha(T)$ dependence.

III. RESULTS

A. Refractive index

The change in the sample temperature T was performed in steps, waiting 15–20 min to stabilize it with an accuracy of ≈1 K, prior to the *nd* measurement. Representative examples of temporal evolutions T(t) and *nd*(t) over an arbitrary selected time interval (≈30 min), in which the *nd* was determined for fixed temperature values, are given for the HPHT sample in Fig. 2. The *nd* data are obtained at the stabilized T using about 45 data-points from LCI and ≈20 records from the thermocouple for 2.5 min, while the temperature was kept stable for about 7 min for one step. Insets in Figs. 2(a) and 2(b) show how small the fluctuations are in $T(t)$ and $nd(t)$ after the T stabilization: the root mean square deviations are $\sigma(T) = 0.12$ K and $\sigma(nd) = 0.022$ μm, respectively.

Figure 3 demonstrates the measured temperature dependence of $nd(T)$ for the CVD and HPHT diamond samples. The optical thickness *nd* increases with temperature in a similar manner for both samples, with almost linear trend at T > 1100 K. The error in the *nd* value is mostly due to the non-flatness of the specimens and the temperature uncertainty. The accuracy of thermocouple reading, including the precision of the microvoltmeter used, was $\sigma_T \approx 5$ K. The axial gradient of temperature $\partial T/\partial Z = 6$ K/mm inside the quartz tube furnace contributed much smaller error (≈1 K) in the measured temperature. The error in the temperature translates into inaccuracy in the measured optical path $\Delta(nd) = \partial(nd)/\partial T \times \sigma_T \approx 0.25$ μm for the HPHT sample and 0.12 μm for the thinner CVD sample. Taking into account the nonparallelism for the HPHT and CVD samples, and a possible shift in the probed position of the LCI beam from the specimen center (less than 0.5 mm), we estimated the maximum errors in the measured change $[nd(T) - nd(300)]$ of ±2 μm (0.09%) for the HPHT sample and ±0.3 μm (0.03%) for the CVD diamond that were smaller than the symbols depicted in Fig. 3.

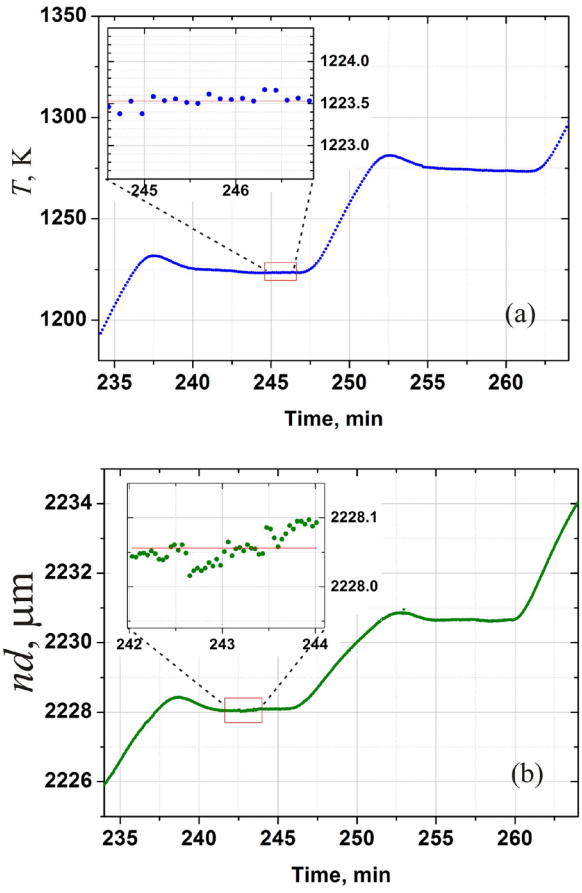

FIG. 2. Examples of measured temporal evolutions T(t) (a) and *nd*(t) (b) during the stepped heating of the HPHT diamond sample (a 30 min part of the experiment with two steps is shown). The *nd* is determined at a fixed temperature after T(t) stabilization. Arrows show the moments of start and end of *nd* evaluation procedure on the T(t) plateau. Insets in (a) and (b) show zoomed $T(t)$ and $nd(t)$ fluctuations for 2 min, respectively, at the stabilized temperature.

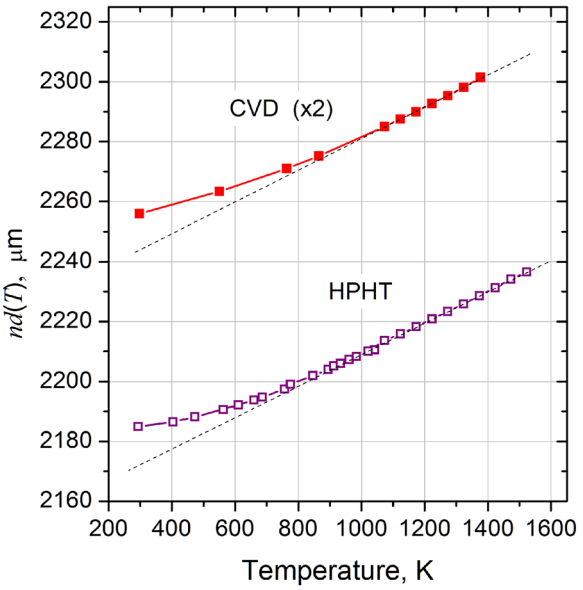

FIG. 3. The plot for measured nd(T) vs. temperature for single crystal HPHT diamond (open magenta squares) and polycrystalline CVD diamond (filled red squares). The plot for the CVD diamond is scaled by ×2 for the picture compactness. The lines are guides for an eye. The error bars of ±4 μm and ±0.7 μm for HPHT and CVD sample, respectively, are smaller than the size of the symbols on the graph. The dashed straight lines are linear fits at high temperatures.

A more universal temperature dependence for *nd*, free from the specimen thickness at 300 K, can be obtained in the form of a relative change of *nd* with respect to its room temperature value[23] $[nd(T) - nd(300)]/nd(300) = [n(T)/n(300)] \times [1 + \langle\alpha\rangle(T–300)] - 1$, where $\langle\alpha\rangle$ is the thermal expansion coefficient averaged over the temperature range from 300 K to T. Figure 4 shows the relative change in *nd* vs. temperature for our two samples, that very well, with an accuracy of $\pm 0.5 \times 10^{-3}$, is described up to 1600 K with the 4th order polynomial

$$[nd(T) - nd(300)]/nd(300) = 4.70 \times 10^{-4} - 9.96 \times 10^{-6} \times T + 3.21 \times 10^{-8} \times T^2 - 1.45 \times 10^{-11} \times T^3 + 2.77 \times 10^{-15} \times T^4. \quad (1)$$

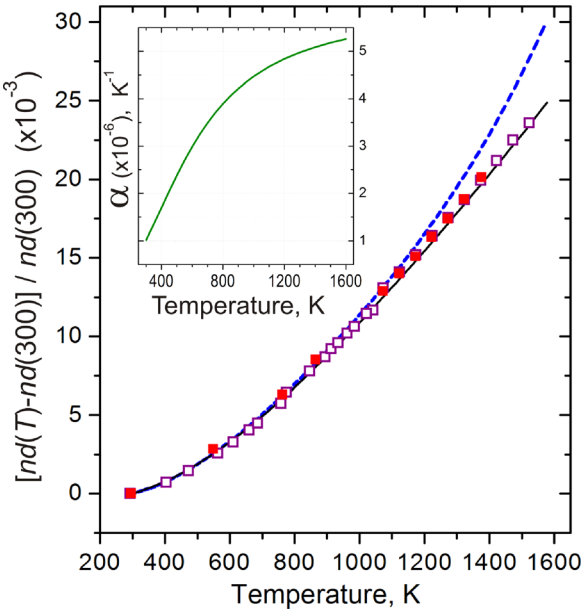

FIG. 4. Relative change $[nd(T) - nd(300)]/nd(300)$ vs. temperature for the HPHT sample (open squares) and the CVD sample (closed squares). The dashed line is polynomial fit [Eq. (2)][23] and solid line is polynomial fit [Eq. (1)], this work. Inset: temperature dependence of thermal expansion coefficient $\alpha(T)$ for diamond.[27]

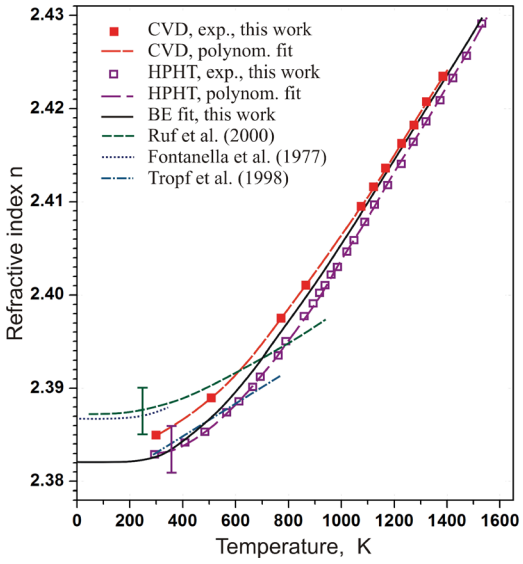

FIG. 5. The temperature dependence of refractive index $n(T)$ for diamond at different wavelengths λ: natural IIa diamond, $\lambda = 100\,\mu$m by Ruf *et al.*[12] (short dashed line); natural IIa diamond, $\lambda \sim 10^{10}\,\mu$m by Fontanella *et al.*[30] (dotted line); polycrystalline diamond, $\lambda = 2.2\,\mu$m by Tropf *et al.*[19] (dashed dotted line); HPHT diamond, $\lambda = 1.55\,\mu$m, this work (open squares); polycrystalline CVD diamond, $\lambda = 1.55\,\mu$m, this work (full squares). The long dashed lines are polynomial fits [Eq. (3)]; the solid line is the fit with Bose-Einstein model [Eq. (4)] common for the CVD and HPHT diamond samples, this work.

Dischler and Wild[23] give a different fit to the experimental data for natural diamond available for these authors up to 800 °C, using also the 4th order polynomial

$$\left[nd(T) - nd(25\,\mathrm{C})\right]/nd(25\,\mathrm{C}) = -8.1 \times 10^{-5} + 3.02 \times 10^{-6} \times \mathrm{T} + 2.91 \times 10^{-8} \times \mathrm{T}^2 - 2.29 \times 10^{-11} \times \mathrm{T}^3 + 9.52 \times 10^{-15} \times \mathrm{T}^4, \quad (2)$$

where the temperature is given in °C. We found their fit to be almost perfect for our measured data till 1000 K, but clearly overestimated at higher temperatures. Therefore, our approximation [Eq. (1)] is valid for a wider temperature range, compared with [Eq. (2)]. The dependences (1) and (2) contain contributions from both $n(T)$ and thermal expansion coefficient for diamond, the latter varied by a factor of five with the temperature increase from 300 K to 1600 K as shown in the inset in Fig. 4.

The refractive index was calculated as $n(T) = nd(T)/d(T)$, where thickness $d(T)$ was corrected to thermal expansion at the particular temperature. As pointed out in Sec. II, due to a significant uncertainty in $d(T)$, that can amount up to ≈5% at $\mathrm{T} > 1300$ K,[27] the accuracy in $n(T) = (nd)(T)/d(T)$ dramatically worsens compared with that for directly measured nd value. This conclusion is valid principally for all versions of interferometry measurement of the refractive index. The dependences $n(T)$ for the CVD and HPHT diamond samples are shown in Fig. 5. The refractive index at room temperature $n(300\,\mathrm{K})$ of 2.383 and 2.385 was determined for CVD and HPHT diamond, respectively. Both samples revealed a very close $n(T)$ behavior, with $n_0 = 2.383 \pm 0.001$ at 298 K, monotonically increasing to 2.428 at 1520 K. Therefore, the 1.8% change ($\Delta n = 0.044$) in the refractive index takes place between 300 K and 1500 K. Note that $n(T)$ increases gradually with T below 400 K, and more strongly above this temperature. Almost linear $n(T)$ dependence is observed above 800 K. A linear approximation of $n(T)$ is expected at temperatures much larger than the Debye temperature Q_D [for diamond $\mathrm{Q}_D = 1860$ K (Ref. 28)] where the vibrational degrees of freedom can be described by a single "effective" phonon oscillator,[12] while Zouboulis *et al.*[22] claimed the linear behavior to occur above (1/2 Q_D), or, roughly at >900 °C for diamond.

Also displayed in Fig. 5 are published experimental data for natural IIa diamond ($\lambda = 100\,\mu$m) by Ruf *et al.*[12] and polycrystalline diamond ($\lambda = 2.2\,\mu$m) by Tropf *et al.*[19] At room temperature, our values $n(300\,\mathrm{K})$ and literature data fall in the narrow range of 2.383–2.387, in spite of a big difference in the wavelengths used, 1.56 μm vs. 2.2 μm and 100 μm, which is a consequence of low dispersion in $n(\lambda)$ in infrared, for wavelengths above approximately 1.5 μm.[11] Note that Hu and Hess[20] reported an abnormally low $n = 2.322$ at $\lambda = 1.03\,\mu$m (not shown here) for a nanocrystalline diamond film, presumably due to an inaccurate thickness measurement of very thin samples (≈0.3 μm).

The $n(T)$ data for two our diamonds are well fitted with the 3rd order polynomial

$$n(T) = n_0 + aT + bT^2 + cT^3, \quad (3)$$

with $n_0 = 2.384$, $a = -2.05 \times 10^{-5}$, $b = 5.49 \times 10^{-8}$, $c = -1.47 \times 10^{-11}$, for the HPHT sample, and $n_0 = 2.380$, $a = 7.47 \times 10^{-6}$, $b = 2.09 \times 10^{-8}$, $c = -2.92 \times 10^{-12}$ for the CVD sample.

The increase in the refractive index with temperature is due to an increased electron-phonon interaction at elevated temperatures.[29] We fitted the $n(T)$ also by Bose-Einstein

(BE) model used by Ruf *et al.*[12] to describe their experiments at a temperature up to 925 K

$$n(T) = n_0 + A\left[n_{\mathrm{BE}}(\hbar\omega, T) + 1/2\right], \quad (4)$$

where n_0 is a constant, A is the dimensionless coupling constant, k is Boltzmann constant, and $n_{\mathrm{BE}}(\hbar\omega,\mathrm{T}) = [\exp(\hbar\omega/k\mathrm{T}) - 1]^{-1}$ is Bose-Einstein factor for the effective phonon frequency $\hbar\omega$ that describes the vibrational degrees of freedom at $\hbar\omega \gg \mathrm{kT}$. We obtained a good common fit for both samples (Fig. 4), with $n_0 = 2.346$, $A = 0.072$, and $\hbar\omega = 970\,\mathrm{cm}^{-1}$, this frequency being 1.36 time larger than $711\,\mathrm{cm}^{-1}$ reported by Ruf *et al.*[12] for the long wavelengths. This particular BE fit is accurate with 0.5% with respect to describing both our experimental curves $n(T)$. Even better individual fits for CVD or HPHT samples can be achieved just by a small change of the common optimum value of A to 0.070 or 0.074, respectively. Note that the phonon frequency of $970\,\mathrm{cm}^{-1}$ found here corresponds to the thermal energy kT at 1700 K, close to Debye temperature $\Theta_{\mathrm{D}} = 1860$ K for diamond. The fit [Eq. (4)] predicts the linear dependence $n(T) = n_0 + (A/\hbar\omega)k_BT$ in high-temperature limit $kT \gg \hbar\omega$ ($T \gg 1700$ K); however, we see almost linear behavior of the measured $n(T)$ already above 1000 K (Fig. 5). Both fits, either with BE model or with polynomials, provide good enough description of our measured data. If extrapolation of $n(T)$ to outside the reported temperature range is needed, the BE fit is preferable, while the polynomials are unreliable below room temperature or above 1600 K. Particularly, the polynomials [Eq. (3)] lead to a decrease of thermo-optical coefficient at $\mathrm{T} > 1600$ K, while the BE model [Eq. (4)] shows a constant value for the thermo-optical coefficient.

B. Thermo-optical coefficient

By differentiating the polynomials, we obtained the temperature dependence of thermo-optical coefficient $\beta(T)$ for each sample, described with the 2nd order polynomials

$$\beta(T) = (1/n)(\mathrm{d}n/\mathrm{d}T) = a/n + (2b/n)T + (3c/n)T^2, \quad (5)$$

where the constants a, b, and c are the same as in Eq. (1) and n is taken at 300 K. Thus, the calculated $\beta(T)$ as a function of temperature is displayed in Fig. 6. Note that we assumed the constant $n = 2.40$ in the denominator of Eq. (5) instead of using the exact temperature dependent $n(T)$, and this simplification results in only a small error in $\beta(T)$, less than 0.8%, across the temperature range explored. The thermo-optical coefficient for the HPHT sample smoothly increases from $0.54 \times 10^{-5}\,\mathrm{K}^{-1}$ at 300 K to $2.17 \times 10^{-5}\,\mathrm{K}^{-1}$ at 1470 K, and, similarly, from $0.71 \times 10^{-5}\,\mathrm{K}^{-1}$ at 300 K to $1.96 \times 10^{-5}\,\mathrm{K}^{-1}$ at 1380 K for the CVD diamond. The dependences approach a constant value at a temperature above ~1300 K. Thus, the difference in the $\beta(T)$ for a single crystal HPHT and polycrystalline diamond over the entire temperature range is less than 10%.

In addition, we calculated the thermo-optic coefficient values by differentiating the Bose-Einstein fit to n(T), given in Fig. 5, and displayed the obtained $\beta(T)$ as a thick solid line in Fig. 6. The *BE*-based $\beta(T)$ curve goes very close to the dependences for CVD and HPHT samples obtained from the polynomial approximation at 300–400 K, and $\mathrm{T} > 1000$ K, but it exceeds both of them for less than 10% at intermediate temperatures. The n(T) and $\beta(T)$ values calculated using the *BE* model are given in Table I. The accuracy around room temperature for n(T) is ± 0.001 and for $\beta(T)$ is about $0.05 \times 10^{-5}\ \mathrm{K}^{-1}$. At high temperatures, the error somewhat increases due to uncertainty in the thermal expansion coefficient value, as discussed above. In particular, we estimate the error $\Delta\beta(T)$ of about 2% at $\mathrm{T} > 1000$ K that is comparable to the 1% error for β at $\mathrm{T} = 925$ K reported by Ruf *et al.*,[12] and 2% at 1000 K in work.[21]

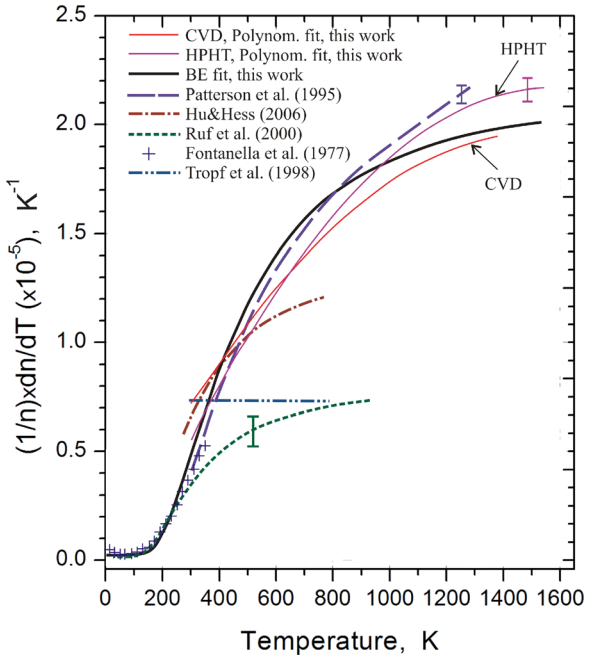

FIG. 6. Temperature dependence of thermo-optical coefficient $(1/n)\ dn/dT$ for diamond according to Patterson[21] ($\lambda = 0.632\,\mu$m, long dashed line); Tropf *et al.*[19] ($\lambda = 2.2\,\mu$m, dashed dot-dot line); Fontanella *et al.*[30] ($f = 10^4$ Hz, crosses); Ruf *et al.*[12] ($\lambda = 100\,\mu$m, short dashed line); Hu and Hess[20] ($\lambda = 1.03\,\mu$m, dashed dot line); HPHT and CVD diamond, this work: experiment (thin solid lines) and Bose-Einstein fit (thick solid lines).The error bars for the data are shown.

TABLE I. Experimental values $n(T)$ and $\beta(T) = (1/n)(\mathrm{d}n/\mathrm{d}T)$ for diamond at different temperatures as determined by Bose-Einstein fitting.

T, K	n	β, $10^{-5}\,\mathrm{K}^{-1}$	T, K	n	β, $10^{-5}\,\mathrm{K}^{-1}$
293	2.383	0.41	961	2.404	1.80
404	2.384	0.85	984	2.405	1.82
473	2.386	1.07	1031	2.407	1.84
563	2.389	1.31	1073	2.409	1.86
610	2.390	1.41	1123	2.411	1.89
660	2.392	1.49	1173	2.413	1.91
686	2.393	1.55	1223	2.416	1.92
757	2.395	1.63	1273	2.418	1.94
775	2.396	1.66	1323	2.420	1.95
846	2.399	1.71	1373	2.423	1.97
894	2.401	1.75	1423	2.425	1.98
912	2.402	1.77	1473	2.427	1.99
933	2.403	1.78	1523	2.430	1.99

TABLE II. Summary of experimental present and literature values $n(T)$ and $\beta = (1/n)(dn/dT)$ for diamond at different temperatures. The temperature range ΔT_{meas} of the measurements is indicated.

Sample type	Wavelength, μm	ΔT_{meas}, K	Method	n (300 K)	n (800 K)	β (300 K), $\times 10^{-5}$ K^{-1}	β (800 K), $\times 10^{-5}$ K^{-1}	References
HPHT	1.56	300–1523	LCI	2.383	2.399	0.54	1.58	This work
CVD[a]	1.56	300–1375	LCI	2.385	2.395	0.71	1.52	This work
Natural,	0.632;	300–1280	Interferometry	n/a	n/a	0.45	1.65	Patterson[21]
Ib HPHT	0.488					0.45	1.8	
IIa natural	100	50–925	Interferometry	2.387		0.32	0.70	Ruf *et al.*[12]
IIa natural	$\sim 10^{10}$ (f $\sim 10^4$ Hz)	5–340	Capacitor	2.387	n/a	0.40	n/a	Fontanella *et al.*[30]
CVD[a]	2.2	293–784	Interferometry	2.383		0.72	0.7	Tropf *et al.*[19]
	10.0					0.66		
CVD[b]	1.032;	300–770	Ellipsometry	2.322	2.335	0.65	1.2	Hu *et al.*[20]
	0.620;			2.345	2.336	0.61	n/a	
	0.413			n/a	n/a	0.52	n/a	
	0.275;			2.53	2.548	0.36	n/a	
Natural	0.514	300–1600	Brillouin scattering	2.429	2.444	n/a	n/a	Zouboulis *et al.*[22]

[a]Polycrystalline CVD diamond film.
[b]Nanocrystalline CVD diamond film.

It is instructive to compare the obtained results with the experimental data for the thermo-optical coefficient from other works that are also shown in Fig. 6. Our data are closest to the temperature dependence $\beta(T)$ from 300 to 1270 K reported by Patterson.[21] Indeed, the maximum deviation of the corresponding curves at 1200 K (see Fig. 6) does not exceed 20%, while the estimated accuracy in our $\beta(T)$ values is about 10%. Also, a good agreement, especially in the range of T = 300–500 K, occurs with the dependence $\beta(T)$ measured by Hu and Hess,[20] who reported 0.65×10^{-5} K^{-1} at 300 K for thermo-optical coefficient for a nanocrystalline diamond film. The plot from Ruf *et al.*[12] agrees well below 300 K with the values reported by Fontanella *et al.*[30] for a long-wave limit (frequency $f = 10^4$ Hz). At room temperature, they reported 0.32×10^{-5} in Ref. 12 and 0.40×10^{-5} K,[30] respectively. Our data considerably exceed, by a factor of two, those from Ref. 12 in the range of 300–925 K. Finally, the $\beta(T)$ data from Tropf *et al.*,[19] while being reasonably close at 300 K, look quite unusual at an elevated temperature, showing virtually no T-dependence. The temperature dependence of thermo-optical coefficient reported by all authors, including the present work, demonstrates an increase of $\beta(T)$ with T, and saturation at a certain level, which, however, is different and varies with the sample grade, wavelength, and measurement method. A compilation of our results and those from other studies is given in Table II.

According to Bose-Einstein model [Eq. (4)] in the high-T limit, the thermo-optical coefficient is $\beta(T) = (A/\hbar\omega)k \cdot n_0$, that gives a factor of 2.8 larger limit for our data compared with that derived by Ruf *et al.*[12] By extrapolating the experimental data from these authors to 1400 K, where $\beta(T)$ is approaching a plateau (Fig. 6), we have a factor of 2.7 difference in the measured thermo-optical coefficients, in excellent agreement with the theoretical estimate.

The thermo-optical coefficient for diamond turns out to be much smaller than for representative semiconductors transparent in the near-infrared (NIR) spectra range. The room temperature (1/n)(dn/dT) values of $(6 \pm 1) \times 10^{-6}$ K^{-1} for near infrared wavelengths reported by Tropf *et al.*,[19] Hu and Hess[20] and the present results are an order of magnitude lower compared with the values measured at $\lambda = 1.53$ μm (close to the wavelength use here) for other semiconductors important for optoelectronics such as Si, GaAs and InP with 5.15×10^{-5} K^{-1}, 6.65×10^{-5} K^{-1}, and 5.95×10^{-5} K^{-1}, respectively.[29] This difference is reduced to 2–3 times only at an elevated temperature (800 K), yet remaining to be significant. Note that the refractive index values (300 K, $\lambda = 1.53$ μm) for Si, GaAs, and InP (3.53, 3.44, and 3.24 Ref. 29) are about 40% larger than that for diamond that lessens by the similar factor the observed difference in the $\beta(T)$ for diamond and these crystals.

The room temperature thermo-optical coefficient, combining the present results at $\lambda = 1.56$ μm and literature data,[12,19–21] versus photon energies E_p is plotted in Fig. 7. The data seem to follow a general trend, β(300 K) increasing with E_p from far infrared to NIR, where a maximum of $\approx 0.7 \times 10^{-5}$ K^{-1} is achieved at $E_p \approx 1$ eV, gradually decreasing toward high energies, up to $\approx$4.8 eV. Our data corroborate

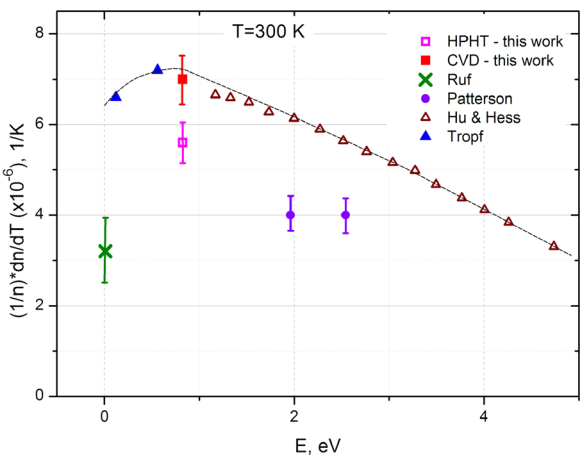

FIG. 7. Experimental dependence of the thermo-optical coefficient at 300 K on photon energy E according to the data reported by Hu and Hess[20] (open triangles), Ruf *et al.*[12] (cross), Tropf *et al.*[19] (full triangles), Patterson[21] (circles), and in this work: HPHT diamond (open squares) and CVD diamond (full squares). The dashed line is a guide for eyes.

TABLE III. The measured thermo-optic coefficient β and tabulated thermal expansion coefficient α for diamond at elevated temperatures.

T, K	β, 10^{-6} K^{-1}	α, 10^{-6} K^{-1} Ref. 27	α/β
300	5.4	1.01	0.19
800	15.8	3.89	0.25
1400	21.0	5.09	0.24

this picture well. The only exclusion is the results, significantly reduced ones, reported by Patterson[21] for the visible spectral range.

As we demonstrated in Fig. 3, the optical path nd for the HPHT diamond sample was measured with a high accuracy of $\approx 0.02\,\mu$m ($\sigma(nd)/nd \sim 10^{-5}$) over the temperature range of 1100–1600 K, where the linear dependence $nd \sim T$ is observed. The sensitivity $d(nd)/dT = nd(\beta + \alpha)$ combines contributions of thermo-optical coefficient β and thermal expansion coefficient α. Table III presents the β values measured by us for the HPHT sample and literature data[27] for α values for room, moderate, and high temperatures. It shows that the thermal expansion provides not more than 25% to the total $nd(T)$ dependence. The change in the optical path $\Delta(\mathrm{nd}) \approx 30\,\mu$m over $\Delta T = 500$ K translates to the temperature sensitivity of 0.06 μm/K, three times exceeding the possible error. This opens a way to use the LCI technique as a thermometry for diamond with an accuracy better than 1 K. We note that the application of LCI to the real-time measurement of Si substrate temperature in the molecular beam epitaxy using low-coherence tandem interferometry was recently reported by Yurasov *et al.*,[31] who claimed the practical accuracy of ± 2 K, and an ultimate accuracy of about 0.1 K.

IV. CONCLUSIONS

We used the low-coherence interferometry to determine the temperature dependence of refractive index $n(T)$ and thermo-optical coefficient $\beta(T) = (1/n)(dn/dT)$ at 1.56 μm wavelength for high purity single crystal HPHT diamond (nitrogen impurity content below 5 ppb) and CVD polycrystalline diamond with a nitrogen content below 1 ppm. The measurements were performed in vacuum in the temperature range from 300 K to 1520 K. Both materials reveal very close optical properties, with $n(300\,\mathrm{K}) = 2.384 \pm 0.001$ increasing to $n = 2.428$ at 1520 K. Almost linear $n(T)$ dependence is observed above 800 K. The accuracy ($\approx 0.09\%$) in the measured normalized increase of optical path $[nd(T) - nd(300)]/nd(300)$ was limited by the nonparallelism of the examined particular specimens. The measured room temperature refractive index turned out to be in excellent agreement with the recent result of Turri *et al.*[32] evaluated for a single crystal CVD diamond using ellipsometry.

The $n(T)$ data can be fitted with accuracy of 0.05% with 3rd order polynomials. We also demonstrate a good fit to the experimental $n(T)$ plots with empirical Bose-Einstein model with an effective oscillator frequency of 970 cm^{-1} that is larger than previously reported by Ruf *et al.*[12] for far infrared wavelengths.

The thermo-optical coefficient $\beta(T)$ as a function of temperature has been determined by differentiating the fits of $n(T)$, and has revealed the increase from $(0.6 \pm 0.1) \times 10^{-5}$ K^{-1} (300 K) to $(2.0 \pm 0.1) \times 10^{-5}$ K^{-1} (1300 K) with a tendency to saturation at >1200 K. At room temperature, the measured $\beta(300\,\mathrm{K})$ values are in a reasonable agreement with previously published results in the near-infrared [wavelengths of 1.03 (Ref. 20) and 2.2 μm (Ref. 19)]. The Bose-Einstein model automatically results in a leveling off the thermo-optical coefficient at high enough temperatures, in accordance with the trend observed in the experiment. The obtained results significantly extend the temperature range, where both the refractive index and thermo-optical coefficient diamond were previously measured, and could be of interest, in particular, for high power laser diamond optics.[6,33]

ACKNOWLEDGMENTS

The authors are thankful to S. G. Ryzhkov for diamond sample polishing and I. A. Antonova and D. S. Plekhanov for data processing. This work was supported by the Russian Science Foundation, Grant No. 14-12-01403-P.

[1]R. J. Williams, J. Nold, M. Strecker, O. Kitzler, A. McKay, T. Schreiber, and R. P. Mildren, Laser Photonics Rev. **9**, 405 (2015).
[2]*Optical Engineering of Diamond*, edited by R. P. Mildren and J. R. Rabeau (Wiley-VCH Verlag, 2013).
[3]T. V. Kononenko, V. G. Ralchenko, E. E. Ashkinazi, M. Polikarpov, P. Ershov, S. Kuznetsov, V. Yunkin, I. Snigireva, and V. I. Konov, Appl. Phys. A **122**, 152 (2016).
[4]S. Terentyev, M. Polikarpov, I. Snigireva, M. Di Michiel, S. Zholudev, V. Yunkin, S. Kuznetsov, V. Blank, and A. Snigirev, J. Synchrotron Radiat. **24**, 103 (2017).
[5]V. E. Rogalin, E. E. Ashkenazi, A. F. Popovich, V. G. Ral'chenko, V. I. Konov, S. M. Aranchii, M. V. Ruzin, and S. A. Uspenskii, Russ. Microelectron. **41**, 464 (2012).
[6]E. Anoikin, A. Muhr, A. Bennett, D. Twitchen, and de H. Wit, Proc. SPIE **9346**, 93460T (2015).
[7]G. Gantenbein, A. Samartsev, G. Aiello, G. Dammertz, J. Jelonnek, M. Losert, A. Schlaich, T. Scherer, D. Strauss, M. Thumm, and D. Wagner, IEEE Trans. Electron Devices **61**, 1806 (2014).
[8]D. N. Sovyk, V. G. Ralchenko, D. A. Kurdyukov, S. A. Grudinkin, V. G. Golubev, A. A. Khomich, and V. I. Konov, Phys. Solid State **55**, 1120 (2013).
[9]B. Dai, G. Shu, V. Ralchenko, A. Bolshakov, D. Sovyk, A. Khomich, V. Shershulin, K. Liu, J. Zhao, G. Gao, L. Yang, P. Lei, J. Zhu, and J. Han, Diamond Relat. Mater. **73**, 204 (2017).
[10]I. Aharonovich, D. Englund, and M. Toth, Nat. Photonics **10**, 631 (2016).
[11]A. M. Zaitsev, *Optical Properties of Diamond: A Data Handbook* (Springer Science & Business Media, 2013).
[12]T. Ruf, M. Cardona, C. S. J. Pickles, and R. Sussmann, Phys. Rev. B **62**, 16578 (2000).
[13]T. V. Kononenko, E. V. Zavedeev, V. V. Kononenko, K. K. Ashikkalieva, and V. I. Konov, Appl. Phys. A **119**, 405 (2015).
[14]S. M. Pimenov, A. A. Khomich, B. Neuenschwander, B. Jäggi, and V. Romano, J. Opt. Soc. Am. B **33**, B49 (2016).
[15]E. V. Bushuev, V. Y. Yurov, A. P. Bolshakov, V. G. Ralchenko, E. E. Ashkinazi, A. V. Ryabova, I. A. Antonova, P. V. Volkov, A. V. Goryunov, and A. Y. Luk'yanov, Diamond Relat. Mater. **66**, 83 (2016).
[16]E. V. Bushuev, V. Y. Yurov, A. P. Bolshakov, V. G. Ralchenko, A. A. Khomich, I. A. Antonova, E. E. Ashkinazi, V. A. Shershulin, V. P. Pashinin, and V. I. Konov, Diamond Relat. Mater. **72**, 61 (2017).
[17]J. Lu, Y. Gu, T. A. Grotjohn, T. Schuelke, and J. Asmussen, Diamond Relat. Mater. **37**, 17 (2013).
[18]Y. F. Meng, C. S. Yan, J. Lai, S. Krasnicki, H. Shu, T. Yu, Q. Liang, H.-K. Mao, and R. J. Hemley, Proc. Natl. Acad. Sci. U.S.A. **105**, 17620 (2008).
[19]W. J. Tropf, M. E. Thomas, and M. J. Linevsky, Proc. SPIE **3425**, 160 (1998).

[20]Z. G. Hu and P. Hess, Appl. Phys. Lett. **89**, 081906 (2006).
[21]M. J. Patterson, "High temperature studies of diamond and CVD diamond thin film," Ph.D. thesis (Rice University, 1995).
[22]E. S. Zouboulis, M. Grimsditch, A. K. Ramdas, and S. Rodriguez, Phys. Rev. B **57**, 2889 (1998).
[23]C. Wild, "CVD diamond for optical windows," in *Low-Pressure Synthetic Diamond*, edited by B. Dischler and C. Wild (Springer, 1998), p. 189.
[24]R. P. Mildren, "Intrinsic optical properties of diamond," in *Optical Engineering of Diamond*, edited by R. Mildren and J. Rabeau (Wiley-VCH Verlag GmbH, 2013), p. 1.
[25]See www.ndtcompany.com for NDT Ltd.
[26]See www.e6cvd.com for Element Six Ltd.
[27]R. R. Reeber and K. Wang, J. Electron. Mater. **25**, 63 (1996).
[28]V. I. Nepsha, "Heat capacity, conductivity and the thermal coefficient of expansion," in *Handbook of Industrial Diamonds and Diamond Films*, edited by M. A. Prelas *et al*. (Marcel Dekker, NY, 1997), p. 147.
[29]J. A. McCaulley, V. M. Donnelly, M. Vernon, and I. Taha, Phys. Rev. B **49**, 7408 (1994).
[30]J. Fontanella, R. L. Johnston, J. H. Colwell, and C. Andeen, Appl. Opt. **16**, 2949 (1977).
[31]D. V. Yurasov, A. Y. Luk'yanov, P. V. Volkov, A. V. Doryunov, A. D. Tertyshnik, M. N. Drozdov, and A. V. Novikov, J. Cryst. Growth **413**, 42 (2015).
[32]G. Turri, S. Webster, Y. Chen, B. Wickham, A. Bennett, and M. Bass, Opt. Mater. Express **7**, 855 (2017).
[33]C. Holly, M. Traub, D. Hoffmann, C. Widmann, D. Brink, C. Nebel, and C. Wenzel, Proc. SPIE **9741**, 974104 (2016).